Research

Ecography 34: 990–1001, 2011
doi: 10.1111/j.1600-0587.2010.06694.x

Subject Editor: Francisco Pugnaire. Accepted 16 October 2010

Environmental modulation of self-organized periodic vegetation patterns in Sudan

Vincent Deblauwe, Pierre Couteron, Olivier Lejeune, Jan Bogaert and Nicolas Barbier

V. Deblauwe (vincent.deblauwe@ird.fr) and J. Bogaert, Lab of Landscape Ecology and Plant Production Systems, Univ. Libre de Bruxelles, 50 av. FD Roosevelt – CP 169, BE-1050 Brussels, Belgium. Present address of VD: IRD-UMR AMAP (Joint Research Unit) botany and bioinformatics of the Architecture of Plants, TA A-51/PS2, FR-34398 Montpellier, France. – P. Couteron, IRD-UMR AMAP (Joint Research Unit) botany and bioinforMatics of the Architecture of Plants, TA A-51/PS2, FR-34398 Montpellier, France. – N. Barbier, Service de Dynamique et Complexité des Systèmes tropicaux, Univ. Libre de Bruxelles, 50 av. FD Roosevelt – CP 169, BE-1050 Brussels, Belgium, present address: IRD-UMR AMAP (Joint Research Unit) botany and bioinformatics of the Architecture of Plants, TA A-51/PS2, FR-34398 Montpellier, France. – O. Lejeune, Faculty of Medicine, Univ. of Antwerp, Campus Drie Eiken, BE-2610 Antwerpen, Belgium.

Spatially periodic vegetation patterns in arid to semi-arid regions have inspired numerous mechanistic models in the last decade. All embody a common principle of self-organization and make concordant, hence robust, predictions on how environmental factors may modulate the morphological properties of these patterns. Such an array of predictions still needs to be corroborated by synchronic and diachronic field observations on a large scale. Using Fourier-based texture analysis of satellite imagery, we objectively categorized the typical morphologies of periodic patterns and their characteristic scales (wavelength) over extensive areas in Sudan. We then analyzed the environmental domain and the modulation of patterns morphologies at different dates to test the theoretical predictions within a single synthetic and quantitative study. Our results show that, below a critical slope gradient which depends on the aridity level, pattern morphologies vary in space in relation to the decrease of mean annual rainfall in a sequence consistent with the predictions of self-organization models: gaps, labyrinths and spots with increasing wavelengths. Moreover, the same dynamical sequence was observed over time during the Sahelian droughts of the 1970s and 1980s. For a given morphology, the effect of aridity is to increase the pattern wavelength. Above the critical slope gradient, we observed a pattern of parallel bands oriented along the contour lines (the so called tiger-bush). The wavelength of these bands displayed a loose inverse correlation with the slope. These results highlight the pertinence of self-organization theory to explain and possibly predict the dynamics of these threatened ecosystems.

At the transition between arid and semi-arid regions (sensu UNEP 1992), spatial heterogeneity of the vegetation cover is commonly seen as a consequence of resource concentration. Vegetated patches accumulate water, erodible soil particles, organic matter and propagules that are carried away from open areas by wind or water runoff (Schlesinger et al. 1990). Such vegetations can reach very high levels of organization, in which landscapes display contrasted spatial distributions of biomass (see reviews of Ludwig et al. 2005, Rietkerk and van de Koppel 2008). They are characterized by either scale independent arrangements (power law) or, conversely, by periodic patterns showing consistent dominant wavelengths and morphologies over extensive areas (Kefi et al. 2007b, Manor and Shnerb 2008, von Hardenberg et al. 2010). Spatially periodic patterns, which will be our focus here, typically appear as two-phase mosaics composed of relatively dense and scarce vegetated patches (i.e. the wavelength thus refers to the unit cycle including a thicket and a relatively barren inter-thicket area) whose components form rounded or elongated units regularly repeated in a matrix dominated by the other component. The most famous example is that of tiger-bush vegetation, where bands of nearly bare soil alternate with dense thickets of grass or shrubs and run along the contour lines.

Recently mechanistic models of self-organization have helped to rationalize the link between eco-hydrologic feedback processes occurring at the local (plant or patch) scale and the emergence of landscape scale periodic patterns (see Borgogno et al. 2009 for a review). These models invoke symmetry breaking instabilities triggered by the spatial interactions between the plants and a limiting resource to explain the emergence of vegetation patterns. Thanks to this approach, gapped and labyrinthine patterns, often found in adjacent areas (Clos-Arceduc 1956, White 1970, Valentin et al. 1999), were first recognized to emerge from the same processes that trigger banded patterning but under different environmental constraints. In this respect, self-organization of the vegetation can be regarded as more realistic than models invoking feedback loops between vegetation and termite nest building (MacFadyen 1950, Clos-Arceduc

1956, Sileshi et al. 2010) or soil and litter redistribution (Bryan and Brun 1999, Eddy et al. 1999) since the latter hypotheses do not predict the complete range of observed morphologies nor their sequence along environmental gradients (see discussion in Deblauwe 2010).

Despite a fair amount of variation in the hypothesized ecological mechanisms and hence in mathematical formulations, most of the self-organization models converge on several fundamental predictions:

P1. All of the regular patterning morphologies reported from semi-arid areas can be produced on the basis of a very parsimonious set of feedback mechanisms, in the form of short range activation and longer range inhibition modulating the local dynamics of water and vegetation (Rietkerk and van de Koppel 2008, Borgogno et al. 2009).

P2a. Under homogeneous and isotropic conditions (i.e. on non-sloping terrain and in the absence of an influential dominant wind), stress (i.e. decreased productivity and/or increased mortality) induced by increasing levels of aridity, grazing or wood cutting provokes a predictable succession of pattern morphologies. Round gaps arranged in a hexagonal lattice (0-hexagons) first appear in the uniform vegetation cover and then elongate and coalesce to form a labyrinthine structure. As the aridity further increases, round spots arranged in a hexagonal lattice (π-hexagons) are the only remnant of the vegetation within a bare soil matrix, preceding a final transition to bare soil (desert) (Lejeune and Tlidi 1999, Couteron and Lejeune 2001, Rietkerk et al. 2002, Meron et al. 2004, D'Odorico et al. 2006, Guttal and Jayaprakash 2007, Lefever et al. 2009). A sketch of model predictions regarding aridity driven pattern modulation is exemplified along the x axis of Fig. 1.

P2b. Lower rainfall (increased aridity) conditions patterns with larger wavelengths (Lefever and Lejeune 1997, Lejeune et al. 2004, Sherratt and Lord 2007).

P3a. In the presence of a sufficient anisotropic environmental influence, e.g. due to ground slope or dominant winds, all the above morphologies are forced into parallel bands elongated in a direction perpendicular to the environmental anisotropy, forming the so-called tiger bush (Lefever and Lejeune 1997, Lefever et al. 2000, von Hardenberg et al. 2001, Rietkerk et al. 2002). A sketch of simulation results illustrating slope driven pattern selection is exemplified along the y axis of Fig. 1.

P3b. As slope steepens, run-off intensifies and the competition range increases in the upslope direction, inducing an increase in the wavelength of banded patterns (Sherratt 2005).

P3c. Bands are predicted to migrate in the upslope direction (Lefever and Lejeune 1997, Sherratt and Lord 2007).

P4. Several self-organization modeling approaches have also pointed to the possibility of hysteresis loops and critical points in the aridity driven succession of vegetation states. Transitions between desert and spotted patterns (Lejeune et al. 2002), between uniform cover and gapped patterns, and among the different pattern morphologies and wavelength may not occur at the same critical aridity levels during drying and wetting phases therefore being dependent on initial conditions (Lejeune et al. 2004, Meron et al. 2004, Sherratt and Lord 2007). In other words, multiple stable vegetation states may coexist within some range(s) on the aridity scale.

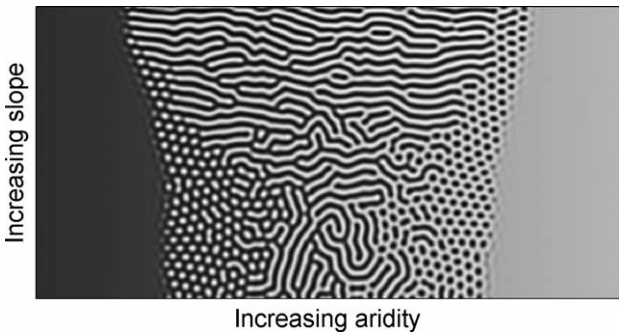

Figure 1. Sketch of model results from a modified version of the Lefever–Lejeune model (Lefever et al. 2009), showing vegetation density as grayscale levels. The simulation was started with a uniform distribution of vegetation states. Vegetation patterns change from uniform cover (black) to gaps, labyrinths, spots and bare soil (light gray) with increasing aridity (increasing along the x axis) and change to parallel bands with increasing slope influence (slope direction is towards the bottom and increases along the y axis). Parameters values are $K=0$; $G=-2$ and M varying between -0.4 and 0.4 (see op. cit. for symbol definition).

Since spotted patterns and desert may represent alternative stable states, several authors have proposed that periodic vegetation may serve as warning signals of imminent and rapid ecosystem collapse or 'catastrophic shift' (Kefi et al. 2007a, Rietkerk et al. 2004).

Regarding P1, we have previously shown (Barbier et al. 2006, 2008) the existence of local scale facilitation and competition mechanisms as well as the absence of a pre-existing blueprint in the substratum in a gapped vegetation pattern, a strong argument in favor of the endogenous nature of the periodic patterning. These field measurements, when used to calibrate an enhanced variant of the self-organization model of Lefever and Lejeune (Lefever and Lejeune 1997), allowed for the simulation of patterns with a similar scale and morphology (i.e. 'deep' gaps) as the natural patterns for which measurements were made (Lefever et al. 2009). Moreover, even though such an explicit linkage between processes measured in the field and the properties of the emerging pattern via a mathematical model has rarely been done, a large body of literature corroborates the existence of local positive and negative feedbacks in arid lands (Schlesinger et al. 1990, Callaway 1995).

Addressing pattern dynamics (predictions P2–P4) in these ecosystems requires using a landscape-to-regional scale approach because the pattern wavelength ranges between tens and hundreds of meters. In fact, the widespread distribution of periodic vegetation patterns only became conspicuous with the advent of the aerial photography in the 1950s (MacFadyen 1950, Clos-Arceduc 1956). Similarly, their slow temporal dynamics are impossible to assess across regions of significant extent without making use of earth observation data. Affordable optical data with very high resolution (either from airborne or satellite sensors) are now increasingly available. They can be found over most semi-arid regions and most often with good temporal hindsight (40 yr or more). At the same time, quantitative methods have been developed to consistently extract pattern characteristics from images of varying quality and resolution. Methodologically, it is therefore feasible to grasp the dynamics of

patterned semi-arid ecosystems over sufficient temporal and spatial scales. Thus, we find ourselves at a defining moment, where predictions produced by a rich theoretical environment now have the possibility to be empirically tested.

The objective of the current contribution was to carry out systematic large scale testing of model predictions regarding the modulation of pattern morphologies along natural gradients of aridity and slope. For this aim, we selected a study area in Sudan where it was possible to simultaneously observe extensive territories covered by all the typical types of periodic morphologies: gaps, labyrinths, spots and bands parallel to contour lines (Koffi et al. 2007, Deblauwe et al. 2008). Fourier-based image analysis techniques, which are relevant to characterize periodic morphologies and compare them to model predictions (Couteron and Lejeune 2001, Thompson et al. 2008), were used and refined to confront the predictions with remote sensing observations. We focused on the abovementioned predictions P2 and P3 that deal with landscape-scale dynamics of periodic systems through space and time. Prediction P3c will be investigated elsewhere in detail. Prediction P4 is notoriously difficult to test (Scheffer et al. 2001) and requires analysis with very large temporal hindsight, but we report some interesting related elements.

Methods

Study area

A typical feature at the transition between the Sudanian savannas and the more xeric Sahelian steppes – hence referred to as the Sudano-Sahelian subzone (Aubréville 1938, Le Houérou 1980) – is the arrangement of vegetation into periodic patterns of decametric to hectometric scale. An area of 22 255 km^2, for which we possess a vertical imagery record, was selected in the Western Sector of southern Kordofan State (part of the former West Kordofan State) of Sudan, ca 700 km south-west of Khartoum (see Fig. 4 for location). Considerable extent of vegetation display there periodic aspects such as parallel bands that sometimes elongate over several kilometers, labyrinthine bands without dominant orientation and spotted and gapped patterns. What we call here 'gapped pattern' has often been referred to as spotted (Valentin et al. 1999, Couteron and Lejeune 2001, Barbier et al. 2006). However, we had to abandon this previous nomenclature to avoid confusion with the reverse patterns of vegetated spots over a matrix of nearly-bare soil. The observable patterns display a wavelength ranging broadly between 40 and 150 m (25 to 6.67 cycles km^{-1}) and can thus be characterized on remote sensing images with a nominal pixel resolution of 10 m, as we did in this study. Examples of typical pattern morphologies in our study area are given in Fig. 2. The reader may also refer to Fig. 1 in Deblauwe et al. (2008).

The area under study lies along both sides of the seasonal stream Wadi El Ghallah at about 180 km SE of the banded patterns described by Wickens and Collier (1971), namely *Terminalia brownii* arcs and *Acacia mellifera* whorls. These patterns were reported to occupy gentle slopes (around 0.5%) where hard soils developed from both the Nubian sandstone series and conglomerates and the Basement Complex outcrops from the thin mantle of Low Qoz sands (Wickens and Collier 1971, Warren 1973). The similar climatic and geological properties in addition to the geographical proximity led us to assume that the vegetation composition and structure of our study area are similar to that reported by these authors. The climate is semi-arid, with a yearly mean rainfall ranging from 370 to 600 mm (TRMM data, see below). Vegetation growth is restricted to the short rainy season running from June to September when 89% of the annual rainfall occurs (rain gauge data, see below). The mean annual rainfall monotonically decreases from SE to NW. This gradient direction is mainly attributed to the orographic lifting effect of the Nuba Mountains in the east (Zahran 1986). Annual rainfall is highly variable over the Sahel region, and a long drought period occurred during the last decades of the twentieth century. Compared to the 1921–1950 average, the rainfall deficit was of 15% during the 1956–1985 interval in central Sudan, and the annual rainfall was persistently low from the mid 1960s up to the end of the 1980s (Hulme 1990). These low yearly figures were caused by a reduction in the frequency of rain events rather than a reduction in the average rainfall yield per rainfall event (Hulme 1990).

The altitude ranges from 400 to 600 m above mean sea level, and most of the area (91%) presents a ground slope of $<1\%$ (SRTM dataset, see below). Few anthropogenic and hydrographic features are observable. Land use consists of shifting cultivation usually hailing from the main settlements: El Muglad, Babanusa and El Fula (mainly concentrated in the NW part). The area under study is browsed during the course of the rainy season, when temporary water ponds are replenished, mainly by transhumant and nomadic pastoralist groups. Average population density for the former West Kordofan State in 2005 was 11 persons per square kilometer with three-quarters living in rural areas (Pantuliano et al. 2009).

Remote sensing data

A synchronic dataset of space-borne images was constructed from seven panchromatic images acquired by the SPOT (Système Probatoire d'Observation de la Terre) sensors with a 10-m ground resolution and preprocessing level 2A. They were acquired on 22 December 2001 and 19 March 2002, that is, during the same dry season. A three-date temporal series spanning a 34-yr period was further built by adding another SPOT image (same quality) acquired on the 3 November 1988 as well as four images from the corona KH-4A reconnaissance satellite system acquired on 19 January 1967, initially on panchromatic films and digitized at a 2.7-m ground resolution (available from the USGS: <http://earthexplorer.usgs.gov>). Corona imagery was resampled to a ground resolution of 10 m to match that of SPOT images. For convenience and comparability with the rainfall time series we will refer in the text to each of the three dates by the year of the preceding growing season: 1966, 1988 and 2001.

Orthorectification procedures were simplified by the flat topography of the area, which allowed for neglecting relief displacement. Each 2001 raw image was initially co-registered to neighboring images to produce a baseline

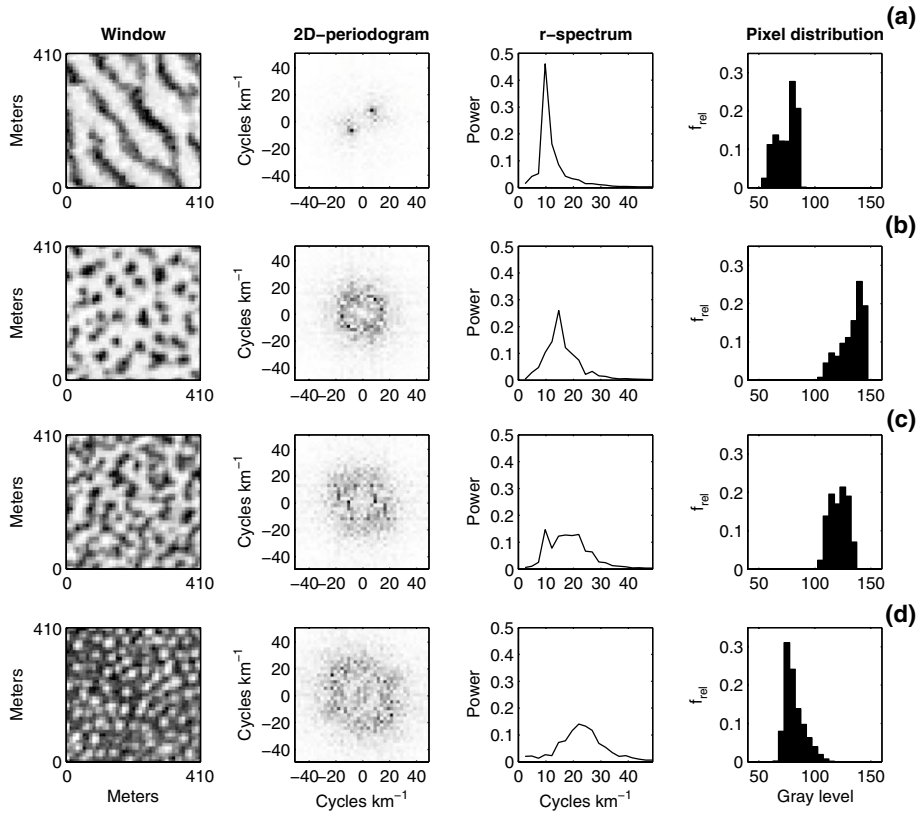

Figure 2. Fourier signature, i.e. two-dimensional (2D) periodogram, r-spectrum and pixel gray level distribution extracted from 2001 SPOT imagery (first column) for representative windows exemplifying each morphology class. Darker tones in the 2D-periodogram express higher amplitudes values. (a) Bands, Ai = 0.62, S = −0.50. (b) Spots, Ai = 0.06, S = −0.82. (c) Labyrinths, Ai = 0.14, S = −0.02. (d) Gaps, Ai = 0.12, S = 1.05, where Ai is the anisotropy index computed from the 2D-periodogram and S is the skewness of the distribution of pixel values. See Fig. 4 for geographic locations of the windows.

mosaic. The diachronic series was subsequently georectified to match the baseline using simple scaling and translation for the 1988 SPOT scene and a third order polynomial adjustment for the 1966 Corona images. Root mean squares of residual adjustment errors were <10 m in the field (i.e. less than one image pixel).

On panchromatic digital images, higher values (bright pixels) usually correspond to bare soil, intermediate gray-scale levels to closed grass cover and lower values (darker pixels) to woody vegetation. In first approximation, gray-scale levels can thus be considered as a monotonically decreasing function of the aboveground biomass (Couteron and Lejeune 2001).

Given the scarcity of available rain gauge station records in central Sudan, the interpretation of synchronic data was made on the basis of the spatial variation of mean annual rainfall assessed using gridded monthly estimates from the Tropical Rainfall Measuring Mission (TRMM, NASA/JAXA) 3B43 V6 product acquired from 1 January 1998 to 31 December 2007. Because the TRMM horizontal resolution is 0.25° by 0.25°, we performed an interpolation between the centers of grid cells (natural neighbors) to match the feature extraction window size (see below). TRMM data perform very well in the absolute rainfall amount estimation in comparison with other satellite-rain gauge mixed estimates in semiarid regions of Africa (Adeyewa and Nakamura 2003). It is reasonable to assume that the rainfall gradient direction evaluated using the TRMM dataset is representative of a very long period and can be used to assess the stable pattern of spatial variation. The annual rainfall series averaged from En Nahud (14°41′N, 28°25′E) and Kadugli (11°00′N, 30°43′E) stations from 1911 to 2005 (Fig. 8c) were used to assess long term temporal averages and variability over the region.

We used the Shuttle Radar Topography Mission (SRTM) digital elevation model with three arc seconds horizontal (ca 92 m in this area) and 1-m vertical spatial resolutions as a topographical reference. The relative vertical accuracy has been reported within ± 6 m for 90% of the data (Rabus et al. 2003). We further computed two relevant topography features for each reference unit window of a chosen size, i.e. 410 by 410 m (see below): steepest slope value (1) and slope azimuthal direction (aspect) (2). By convention, the slope aspect is defined as the direction of steepest decrease in altitude. It ranges between 0° and 360° (0° being the north and values increasing clockwise). Superposition of the digital elevation model onto the SPOT mosaic was achieved by scaling and translation with a root mean square residual of <30 m in the field.

The projection and datum for all datasets used or produced were UTM zone 35 N, WGS 1984.

Feature extraction

To characterize the morphological properties of vegetation patterns, the study area was divided into non-overlapping square windows of 410 by 410 m. This size was deemed a good compromise considering the necessity to both correctly characterize patterns with large wavelengths (sometimes >100 m) and avoid heterogeneity in terms of wavelength or morphology within the windows. The two-dimensional (2D) fast Fourier transform and the associated computation of the 2D-periodogram were applied to each window. We give, as an illustration, Fourier signatures for each morphological type in Fig. 2. The use of the periodogram is recommended in the case of patterns showing spatial periodicity. Indeed, its amplitude values express the proportion of the image variance accounted for by sine and cosine functions of explicit spatial frequencies and orientations (Couteron and Lejeune 2001). Correction of radiometric variability between dates is not required because periodogram amplitude values are invariant to linear rescaling of grayscale levels.

The 2D-periodogram (Fig. 2, second column) is a set of gridded values representing the proportion of image variance for each combination of frequency values taken along the Cartesian axes, or equivalently, in polar coordinates, for a given wavenumber (r) and direction (θ). The periodogram is symmetric about the origin because the proportion of variance accounted for by a given wavenumber in one direction is the same in the opposite direction. Hence, a banded pattern, corresponding roughly to a 2D sine or cosine wave (Fig. 2a, first column), will show a single peak for some frequency or frequency range, symmetric in the opposite direction across the origin (Fig. 2a, second column). Isotropous structures, which present the same dominant scale in several directions, i. e. gaps, labyrinths and spots (Fig. 2b–d, first column), show a typical ring of higher contributions in the 2D periodogram (Fig. 2b–d, second column).

Pattern information relative to the sole spatial frequency (scale features) was summarized by summing the periodogram values within ring-shaped concentric bins of unit width (Renshaw and Ford 1984). The resulting radial spectrum (r-spectrum) thus quantifies the contribution of successive ranges of spatial frequencies to the image variance across all orientations (Fig. 2, third column). As a function of the chosen window size and of the image resolution, the analysis was limited to the first 20 wavenumbers (i.e. spatial frequencies smaller than 49 cycles km^{-1} or wavelengths above 20 m) to avoid aliasing effects. We then applied a standardized principal component analysis (PCA) on the whole set of r-spectra ($n = 132\,388$ analyzed windows) with the frequencies taken as variables (Couteron 2002, Couteron et al. 2006). This approach can identify the main textural gradients in the windows dataset in terms of coarseness-fineness and the intensity of the patterns. In this kind of analysis, one may expect to have most of the textural variation accounted for by the first plane of the PCA (Couteron et al. 2006). We chose to extract specific features, namely the azimuthal angle in the first PCA plane, which directly correlates with the dominant frequency in the windows (see Results and Couteron et al. 2006), and the distance from PCA origin, which expresses the degree of scale dominance (Barbier et al. 2010).

Pattern orientation features were extracted from the 2D-periodogram, within the frequency ring characterizing periodic vegetation patterns, i.e. between 6 and 25 cycles km^{-1} (40 to 167 m), to exclude anisotropy sources resulting from large scale gradients or small scale anthropogenic features. Because 2D-periodogram amplitude values are symmetric about the origin, the extracted orientation features are of an axial nature (sensu Fisher 1993). This means that if one wishes to obtain the dominant orientation of the periodogram entries, which can be seen as a set of vectors characterized for a given frequency by their orientation and periodogram value, one cannot simply compute the resultant vector. Indeed, because of the symmetrical nature of the data, the norm of the resultant will always be zero. The solution is then to work only on the periodogram values comprised within $[0–\pi]$ and to double all angles prior to the vector sum computation (op. cit. p. 37). Using this procedure we computed the average pattern orientation in each window as well as the norm of the resultant axis, which was used as an index of pattern anisotropy after division by the sum of periodogram amplitudes to ensure bounding between zero and one. For a given window, a value of one indicates that all the periodogram contributions to the total variance of the frequency ring are concentrated in one particular direction (perfect anisotropy, i.e. parallel straight bands), whereas a value of zero is obtained when angular contributions are equal in several or all directions (isotropy).

Finally, we characterized the relative dominance of vegetation over bare soil by computing the skewness of the grayscale distribution of each window: windows dominated either by bare ground, such as spotted morphologies, or by the vegetation component, such as gapped morphologies, present left-skewed (negative skewness, Fig. 2b) and right-skewed (positive skewness, Fig. 2d) distributions, respectively. Labyrinthine patterns are expected to have a nearly symmetric gray level distribution about the mean (Fig. 2c). Because the skewness value is not affected by linear transformation, this approach does not require the correction of radiometric variability between dates and sensor types.

To summarize, each window was characterized by a set of five features: 1) pattern intensity and 2) dominating spatial frequency (from the ordination of r-spectra), 3) average pattern orientation and 4) anisotropy (circular statistics from the 2D-periodogram), and 5) relative dominance of vegetation over bare soil (skewness from the histogram of gray-levels).

Supervised classification of vegetation patterns

A training set of 1000 windows (of 410 by 410 m) was picked at random for each of the three acquisition dates, and pattern attachment to the relevant morphology class was determined by visual appraisal. Training windows were then used to compute feature thresholds, minimizing classification errors in the following decision tree (Fig. 3): 1) isolation of periodic vegetation patterns corresponding to a dominant frequency in the characteristic range of 6.72 to 24.89 cycles km^{-1} (wavelengths of 40.2–148.8 m), 2) distinction between anisotropic and isotropic patterns via an anisotropy index threshold of 0.2, and 3) separation of spots, labyrinths and gaps among isotropic patterns.

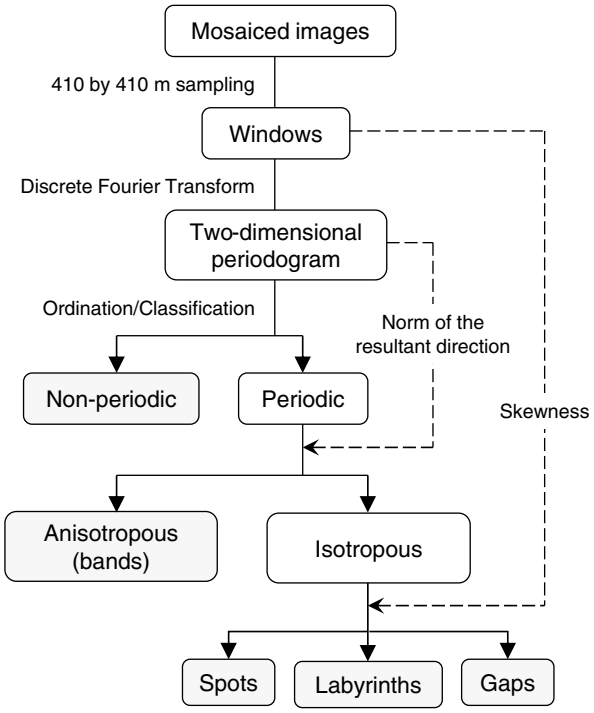

Figure 3. Flow of operations and decision tree for the classification of pattern morphologies.

Results

Classification results

Supervised classification of 2001 SPOT imagery on the basis of the decision tree led to the map shown in Fig. 4. Vegetation patterns covered 13%, i.e. 2866 km^2, of the area under study. Classification results for a sub-sampled area at multiple dates are shown in Fig. 8a. Cohen's kappa coefficient (Cohen 1960) estimating the overall accuracy between the training set of windows and their manually attributed classes reached 0.68 ± 0.03, 0.78 ± 0.06 and 0.68 ± 0.07 (kappa $\pm$ 95% confidence interval), respectively, for the full 2001 and sub-sample 1988 and 1966 classifications, indicating a fair classification performance.

Spatial modulation of pattern morphology

The spatial distribution of each morphology class is strongly zonal, suggesting modulation by physical factors. The bivariate density distribution of morphologies with respect to ground slope and mean annual rainfall are shown in Fig. 5. Banded patterns (anisotropic) appear to be restricted to gently sloping terrains (i.e. between 0.25 and 1%). Conversely, the nearly flat portions of the area (i.e. below 0.25%) only feature gapped, labyrinthine and spotted patterns (isotropic). These results demonstrate that patterns of adjacent areas can vary according to slope intensity. As an illustration, classification results of adjacent windows featuring gapped, labyrinthine and banded patterns along a topographic transect are shown in Fig. 6.

Moreover, slope and aridity effects interact to some extent; the slope threshold conditioning the transition between gapped and banded patterns increases with higher rainfall so that above ca 475 mm of yearly rainfall only gapped patterns develop regardless of slope intensity. Below 400 mm, at the opposite end of the humidity gradient, bands tend to split up into spots and loose anisotropy. Isotropic pattern classes present a NW-SE zonation consistent with the regional gradient in annual rainfall (Fig. 4). Under decreasing rainfall, we observe the following pattern sequence: gaps, labyrinths and spots. The limit between the two latter classes is well-delineated and follows the 400-mm isohyet (Fig. 4, Fig. 5) approximately, whereas the limit between the two former ones is less clear-cut and occurs around 450 mm. The most arid extension of the spotted pattern cannot be assessed because our imagery dataset does not cover areas with <360 mm rainfall.

Spatial modulation of pattern wavelength

We found each morphology class to be characterized by a different frequency mode (Fig. 7) in the following sequence: 12 cycles km^{-1} (wavelength of 83 m) for the bands, 15 cycles km^{-1} (67 m) for the spots, 17 cycles km^{-1} for the labyrinths (59 m) and 24 cycles km^{-1} (42 m) for the gaps. Misclassified gapped patterns explain the presence of an occasional second mode of lesser importance for labyrinthine and banded patterns.

We studied the effect of climate and slope on the spatial frequency of patterns using multiple least squares regression. Box–Cox power transformations of predictors and response variables were applied to comply with normality requirements prior to analysis (Box and Cox 1964). The results are shown in Table 1. Within each pattern morphology class we found a significant positive correlation between spatial frequency and mean annual rainfall ($p < 0.001$). In the case of banded and labyrinthine patterns, the frequency was also positively correlated with the slope gradient ($p < 0.001$). However, the intensity (slope) of this effect was twice as marked (and the R^2 statistic much higher) for the banded patterns. The results indicate that banded patterns tend to have a smaller wavelength under either higher rainfall or steeper slope contexts. When compared with other morphologies, the frequency of banded patterns was more sensitive to slope and less to rainfall.

Temporal modulation

Thanks to the availability of imagery acquired at multiple dates (1966, 1988, 2001), we performed a diachronic analysis of pattern modulation on 4264 windows (ca 715 km^2). Classification results at each temporal step are shown in Fig. 8a with the corresponding annual rainfall series. Owing to its very flat topography, the area was nearly devoid of banded pattern. If we first examine the broad features shown on these maps, we observe that at all dates, spotted patterns dominate in the northwest and labyrinthine patterns in the southeast. The geographical limit between these two classes is quite clear-cut at each date, but its location appears to progressively shift towards the south-east (in agreement to the rainfall gradient) as all morphologies gradually convert to spotted pattern. In the center of the study area, however, localized spotted areas present in 1966 converted to

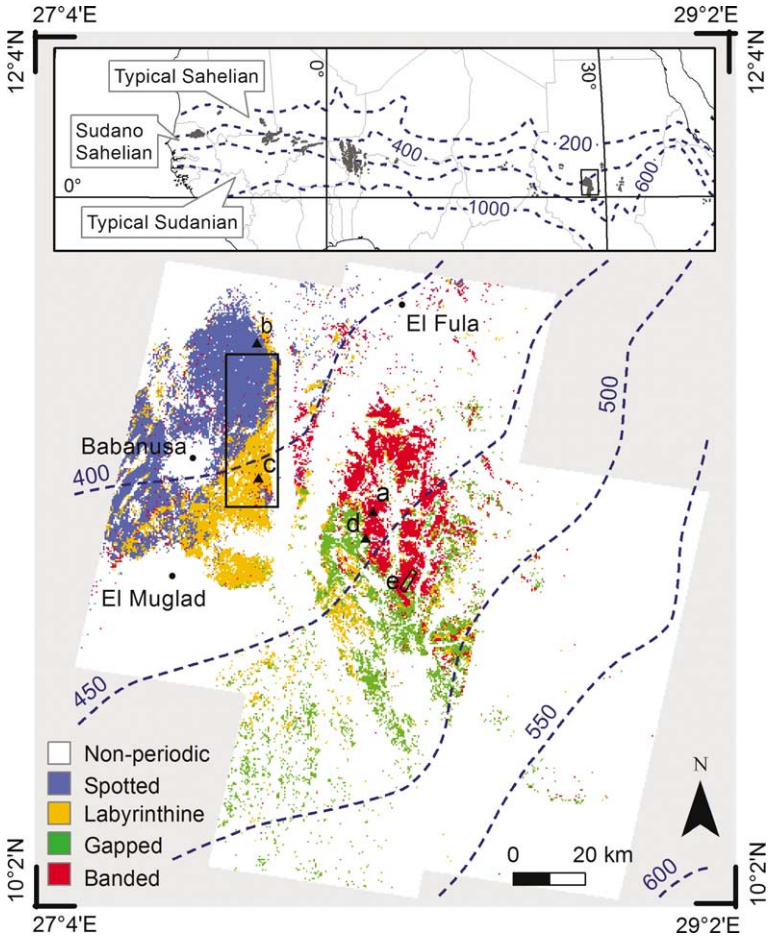

Figure 4. Location of the study area and map of vegetation pattern morphologies computed from the SPOT satellite imagery acquired in 2001. Dashed blue curves represent isohyets (mm) averaged over the period 1998–2007 from TRMM dataset (see text). Insert: geographic location of the study site (black frame) with respect to areas of periodic vegetation patterns (gray areas, adapted from Deblauwe et al. 2008) and ecological zones delimited by 200, 400, 600 and 1000 mm isohyets (Aubréville 1938, Le Houérou 1980). Main panel: black frame shows the coverage of diachronic imagery shown in Fig. 8. The symbols ▲ a–d indicate the respective locations of the windows shown in Fig. 2a–d, and e is location of the profile in Fig. 6. The area outside the 2001 SPOT satellite imagery coverage is shown in gray.

labyrinths in 1988 before returning again to spots in 2001. In addition to pattern modulation induced by variations in the physical environment, anthropogenic pressure is visible around cities. Within a radius of six to eight kilometers around the city of Babanusa, vegetation was mostly spotted by 1966 (data not shown) and was depleted before 2001. Other cities were located far from periodic vegetation areas and had no obvious modulation effect. Except in that particular case we did not observe substantial transition to uniform bare ground.

We will now look in more detail at the window-wise transitions between pattern morphologies while considering only the class transition rates differing significantly (at $p < 0.001$) from the expected values under the null hypothesis of independence between observational periods and transition types according to the Sokal and Rohlf critical values on Freeman–Tukey deviates (Sokal and Rohlf 1995). The three temporal snapshots delimit two successive periods that we analyzed for pattern transition: 1966–1988 and 1988–2001. The first period began immediately after a pluri-decadal episode of above normal precipitations and was characterized by a multi-year period of drought that culminated in the mid 1980s (see the rainfall time series in Fig. 8c). The principal changes concerned transitions from non-periodic vegetation to either gapped or labyrinthine patterns, which affected 12 and 37% of the initially non-periodic windows, respectively. In other words, bare soil patches with a periodic pattern appeared in half of the windows initially displaying uniform vegetation. Moreover, 48% of the gapped vegetation became labyrinthine but without any substantial change in the pattern wavelength. The second period was characterized by annual precipitations closer to the long term average but still lower than the very wet period preceding 1966. Labyrinthine patterns developed over 29% of the vegetation that was non-periodic in 1988. Most of the gapped patterns (89%) became labyrinthine, and nearly half of the labyrinthine patterns (41%) became spotted. These two transition types were accompanied by a decrease in mean spatial frequency: from 23.61 to 18.50 cycles km^{-1}, that is to say from 42.4 to 54.0 m in wavelength ($n = 324$, $p < 0.001$; paired t-test) and from 18.98 to 16.28 cycles km^{-1}, i.e. from 52.7 to 61.4 m ($n = 643$, $p < 0.001$; paired t-test), respectively. These values are consistent with the different frequency modes observed in the synchronic study. For the two periods, vegetation

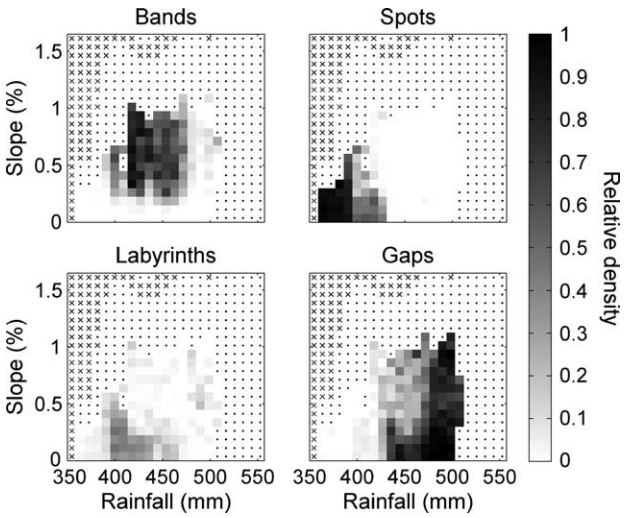

Figure 5. Relative density distribution of pattern morphologies (according to 2001 SPOT imagery) as a function of slope (SRTM data) and mean annual rainfall (TRMM data). Grayscale level is proportional to the relative density among the four pattern morphologies. Dotted areas represent the parameter domain where vegetation is not organized into periodic pattern (less than ten windows featuring periodic vegetation pattern per bin). The domain outside image coverage (less than ten exploitable windows per bin) is shown as crossed area.

encroachment (i.e. transition in the direction spotted > labyrinthine > gapped) were not significantly different to or less frequent than the expected rates under the null hypothesis. As an illustration, the transition sequence from a mixed cover of uniform vegetation and gapped pattern in 1966 to a pure gapped pattern in 1988 and then to a labyrinthine pattern in 2001 is exemplified in Fig. 8b. These detailed statistics therefore confirm the general features presented above, namely of a progressive Southward shift of the different pattern transition limits in concordance with increased aridity conditions (see maps in Fig. 8a).

Discussion

Aridity level

The discrete classification of vegetation into four classes of periodic patterns (and one for non-periodic vegetation) allowed us to show that along a spatial gradient of increasing aridity, the succession of patterns occurred in the order predicted by self-organization models, confirming prediction P2a, namely non-periodic, gapped, labyrinthine and spotted, in this order (see map in Fig. 4). Moreover, during the persistent drought that struck the Sahel during the last three decades of the century, we observed diachronically that transitions occurred along the same sequence (see maps and illustrations in Fig. 8). Both spatial and temporal transitions also corresponded to an increase in wavelength correlated

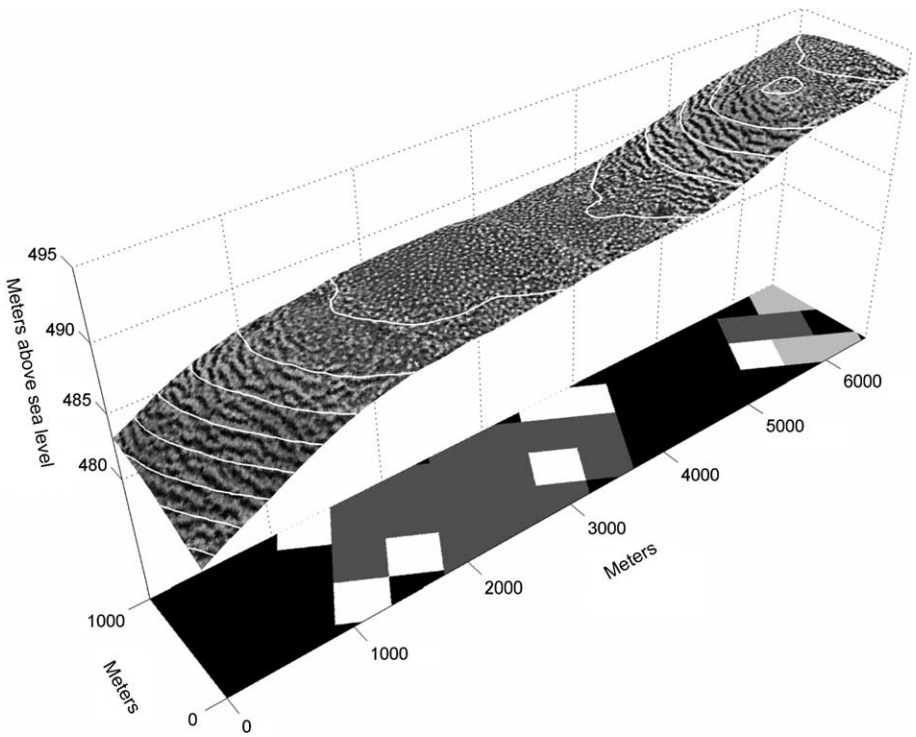

Figure 6. Topographic profile illustrating the transition from fairly isotropic (gapped and few labyrinthine) to anisotropic (banded) patterns as the slope gradient increases. Here, the anisotropic and isotropic areas correspond respectively to slopes mostly in the ranges of 0.25–0.65% and 0.03–0.11%. One-meter contour levels are shown as white curves. We created this artificial view using the SRTM altitude above mean sea level, smoothed by a 200 m moving average window, overlaid with the 2001 SPOT imagery. The vertical scale is exaggerated for visualization purposes. The gridded plane at the bottom indicates the classification results for 410 by 410-m windows: bands (black), gaps (dark gray), labyrinths (light gray) and non-periodic (white). See location in Fig. 4.

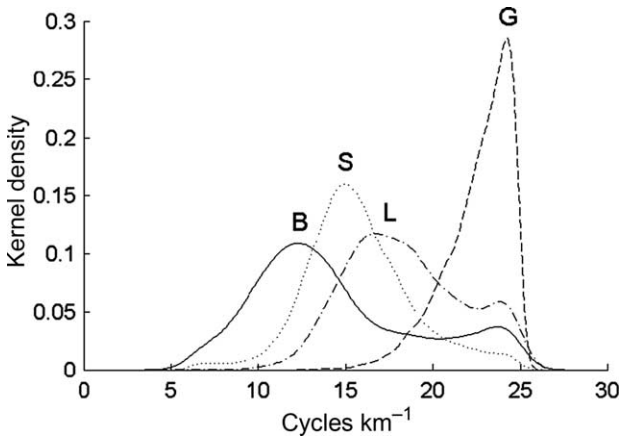

Figure 7. Statistical distribution of spatial frequencies (kernel density) for the main types of periodic vegetation patterns observed in the study area in the Southern Kordofan state of Sudan. B, bands; S, spots; L, labyrinths; G, gaps.

to the increase in aridity, and each class was characterized by a different wavelength mode as predicted in P2b. These dynamics demonstrate that the observed patterns are not fossil structures but rather continue to adjust to fluctuating climatic conditions.

Diachronic analysis gives some clues regarding the timescales involved in the observed pattern modulation dynamics. Indeed, the pattern transitions (gapped to labyrinthine to spotted) observed between 1966 and 1988, during a Sahelian drought period, were still in progress during the closer-to- normal climatic conditions of the 1990s (Fig. 8c). This result does not necessarily contradict the theory, but rather suggests a notable inertia in the vegetation response due to the important perennial component (shrubs) and to the buffering effect of facilitation within thickets (Garcia-Fayos and Gasque 2002). A noticeable inertia in the patterning dynamics has also been documented in Niger, where the thicket to bare soil surface ratio was best correlated with a rainfall averaging period of 15 yr (Valentin and d'Herbès 1999). Our results contrast with other studies based on the normalized vegetation index (NDVI) computed on medium to low resolution satellite images, which either show an absence of change or an increase of the photosynthetic activity over the Sahel from the mid 1980s to the turn of the century (Anyamba and Tucker 2005, Olsson et al. 2005). This paradox underlines that the spatial redistribution/concentration of the biomass occurring at decametric scales may remain hidden to medium resolution vegetation indices.

Human induced pressures may produce different temporal/spatial dynamics than those observed for the sole climate change, either more rapid in the case of continuously increasing population levels (Barbier et al. 2006), or even reverse when this pressure is suddenly alleviated. In parts of our study area close to the Babanusa city, we indeed observed that very limited areas of spotted and labyrinthine patterns present in 1966 shifted to labyrinthine and gapped patterns, respectively, by 1988, in the middle of a multi-year drought and in apparent contradiction to prediction P2a. However, such a change of vegetation patterning towards morphologies interpretable as less marked by aridity happened in conjunction with the desertion of fields and villages following the terrible famines that struck the region in 1972–1973 and 1984–1985 (Olsson and Rapp 1991, Olsson 1993, Olsson et al. 2005). Human death rates are indeed estimated to have reached 3% of the population per month between June 1984 and May 1985, and 2.5 million people migrated to towns or to wetter areas further south (Ibrahim 1988).

Isotropic patterns presented here, i.e. gapped, labyrinthine and spotted, have not yet been reported outside Sub-Saharan Africa. Even there, before the recent introduction of self-organization models (Lefever and Lejeune 1997, Lejeune and Tlidi 1999, Lejeune et al. 1999) along with techniques for detecting spatial periodicity (Couteron and Lejeune 2001), accurate reports were scarce since those patterns were considered to be devoid of meaningful structure, and hence the term 'fuzzy pattern' has often be used (Valentin et al. 1999). Moreover, the spotted vegetation pattern included in our gradient was the first to be reported at the most arid limit of a periodic pattern area (Deblauwe et al. 2008). Therefore, published observations are lacking to allow for the establishment of the generality of our results regarding the succession of isotropic morphologies, although partial evidence has been reported in SW Niger. There, gapped patterns were observed to emerge in previously uniform savannas as the result of either or both increased aridity and human pressure (Barbier et al. 2006). In the same area of Niger, we also observed temporal transitions from gapped to labyrinthine patterns (unpubl.). This finding suggests the generality, at least within the Sudano-Sahelian ecoclimatic belt, of vegetation structure modulation in response to changing aridity levels despite the variety of plant species involved. Furthermore, observations of a wavelength modulation along aridity gradients has already been described qualitatively in the case of banded patterns in SW Niger (White 1970) and Western Australia (Mabbutt and Fanning 1987), thus supporting the generality of prediction P2b.

Overall, our results indicate that mean annual rainfall is a relevant working measure of aridity at the scale of our

Table 1. Multiple linear regressions between the dominant spatial frequency (cycle km^{-1}) in each morphological class as a function of mean annual rainfall (mm) and slope (%). B is the slope coefficient of the regression line, and SE (in brackets) its standard error.

Morphology class	Predictor	B (SE)	t-value	p-value
Bands	Rainfall	0.42 (0.02)	20.76	<0.001
(R^2 =0.22, n =1949)	Slope	0.25 (0.02)	12.71	<0.001
Spots	Rainfall	1.10 (0.32)	3.42	<0.001
(R^2 =0.06, n =6676)	Slope	−0.002 (0.04)	−0.05	0.960
Labyrinths	Rainfall	2.74 (0.26)	10.42	<0.001
(R^2 =0.047, n =2533)	Slope	0.12 (0.02)	5.93	<0.001
Gaps	Rainfall	7.79 (0.49)	16.05	<0.001
(R^2 =0.058, n =4658)	Slope	0.07 (0.03)	2.19	0.629

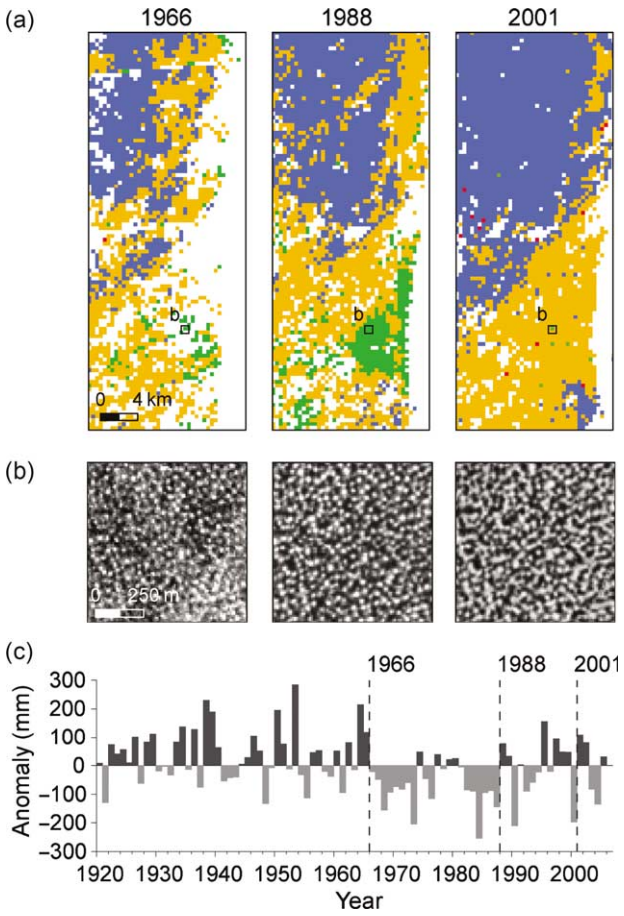

Figure 8. Vegetation pattern dynamics on a pluri-decadal time scale. (a) Diachronic series of classified morphologies for a portion of the study area: bands (red), gaps (green), labyrinths (orange), spots (blue), and non-periodic (white). See location in Fig. 4. (b) Diachronic series of a 0.8 by 0.8-km subset embodying a pluri-decadal transition from a mixed cover of uniform vegetation and gapped pattern to a labyrinthine pattern. Dense thickets appear in black, whereas the bare soil appears in lighter tones. To ease inter-date comparison, each image grayscale was independently linearly stretched with a 1% saturation. The ground location of (b) is delineated by a black frame on the maps in (a). (c) Mean annual rainfall deviations from the 1920–2005 period average (557 mm) at En Nahud and Kadugli rain gauge stations. Photography acquisition dates are indicated by dotted lines.

study area. Nonetheless, the factor causing the northwest-southeast pattern sequence may well include other climatic aspects which are correlated to the mean annual rainfall. For instance, at the global scale we previously showed that potential evapotranspiration (PET), which varies in a direction opposite that of the annual rainfall in the Sahelian climatic belt, has to be taken into account to correctly predict pattern occurrence (Deblauwe et al. 2008). However there is no clear gradient of mean, maximum and minimum temperature at this spatial scale (MODIS Land Surface Temperature data computed over the 2001–2009 period) and the warming trend in central Sudan between the 1940s and 2005 is weak when compared to rainfall fluctuation (Elagib 2010). Rainfall and temperature variability, are likely to be relevant as well, as suggested by both theoretical and empirical evidence (D'Odorico et al. 2006, Guttal and Jayaprakash 2007, Deblauwe et al. 2008) but no consistent seasonality trend was observed during the last decades (Elagib 2010, in press). Assessing the relative influence of these variables will require higher temporal resolution and coverage of vegetation dynamics record.

Topography

Banded and isotropous patterns are often found in close vicinity. Indeed, under a given aridity level, a critical slope gradient threshold exists (ca 0.25% in the area under study, Fig. 5) above which the pattern aligns along the contours into parallel bands, confirming prediction P3a. In a previous study in the same area, we showed that bands were indeed oriented perpendicularly to the slope but with a small, yet significant deviation towards the direction of dominant winds (Koffi et al. 2007). Figure 6 exemplifies such slope-triggered transitions along with the tight correspondence between contour lines and band orientation.

We found the critical slope threshold to be a function of yearly rainfall. In other words, under higher rainfall a steeper slope gradient is required to trigger pattern alignment, and therefore isotropic patterns become more widespread so that above ca 475 mm of yearly rainfall only gapped patterns develop regardless of slope intensity. The increase with higher rainfall of the slope threshold conditioning the pattern alignment provides another supporting evidence for self-organization models (see the generic simulation in Fig. 1). This phenomenon seems to be quite general and has also been observed when combining slope and rainfall data to explain the occurrence of banded patterns in Niger, Sudan and Australia (Valentin et al. 1999). During drought periods, one should therefore observe the coalescence of bare gaps into bands on the steepest slopes. We did not have the opportunity to check for such transitions due to the very flat nature of the terrain in the diachronic study area, but, in another Sahelian zone, Serpantié and colleagues (1992) reported such an effect as a consequence of persisting drought and human pressure.

We found the wavelength of banded patterns to be inversely related to ground slope, thus contradicting the prediction that longer wavelengths will be found on steeper slopes (P3b rejected). However, this observation should be taken with caution because, in our study area, higher slope gradients are predominantly found on intermediate position in the toposequence. It is therefore difficult to discard possible confounding factors linked to wind and/or water erosive processes. Moreover, the overlapping distributions of morphological types along the aridity gradient and the local variations in pattern wavelength suggest the likely influence of edaphic conditions, in particular soil depth and water storage capacity, which were not included in our analysis because of the lack of appropriate soil maps at a relevant scale. However, the inverse relationship between wavelength and slope gradient is supported by observations of banded patterns in Niger and Australia (d'Herbès et al. 1997, Eddy et al. 1999). Further modeling efforts are needed since these interactions between slope and aridity effects on pattern properties have, to our knowledge, not yet been comprehensively investigated in the theoretical literature.

Multiple stable states and criticality

Although we did not seek hysteresis loops and critical points in the aridity driven modulation of periodic patterns, such non-linear dynamics are repeatedly predicted by self-organization models (P4). The discrete nature of the classification scheme we used does not allow us to test whether the full range of intermediate patterns exists between the typical morphological classes or if transitions occur abruptly. This question could be addressed by looking for threshold effects over the phytomass (possibly estimated through the skewness of the gray levels histogram) instead of class dynamics. The use of patterning morphology as bio-indicators or early warning signals of imminent desertification seems difficult to implement, given our observation that spotted patterns did not disappear even during prolonged drought spells, and the strong possibility of a time-lagged or gradual response of the vegetation cover to climate variations. In some instances, we even observed reappearances of spotted morphologies in previously cultivated fields, a fact that contradicts prediction P4 concerning a supposed alternative stable state. Concerning pattern wavelength dependence on aridity level and slope gradient (Table 1), the low R^2 values may be the result of unconsidered local soil variations, but may also be interpreted in the light of the theoretical prediction that several wavelengths may be stable for a given set of aridity and slope conditions (Sherratt and Lord 2007). Both criticality and hysteresis loops should be addressed in dedicated studies based on diachronic remote sensing data supported by field measurements of the soil-vegetation interface.

Conclusions

Within an extensive area in the Southern Kordofan state of Sudan, we found that the regional distribution of several distinct periodic pattern morphologies is related to slope intensity and mean annual rainfall, a fact that strongly supports self-organization theory because symmetry-breaking models have consistently predicted this qualitative modulation of pattern morphologies by these environmental constraints.

More precisely, in the light of the predictions recalled at the beginning of the paper, we can confirm through both synchronic and diachronic approaches that the isotropic morphologies changed from gaps to labyrinths and eventually to spots under increasing aridity (prediction P2a verified). The timescale of pattern modulation, and therefore the appropriate monitoring windows, appeared to be in the order of decades. The succession also corresponded to an increase in wavelength (P2b validated). With regards to the banded morphology, we can clearly evidence the existence of a slope threshold triggering the transition between isotropic and anisotropic morphologies (P3a validated). The critical slope value above which isotropous pattern morphologies convert to parallel bands varies with the mean annual rainfall, and seems to disappear under milder aridity conditions. The banded pattern wavelength is directly proportional to the level of aridity (P2b validated) but varies negatively with the slope gradient, thus invalidating P3b.

These results should help in the continued effort towards quantitative modeling of arid vegetation dynamics, their response to anthropogenic constraints and their interactions with the regional climate, soil and hydric resources.

Acknowledgements – We wish to thank R. Lefever whose work and collaboration stimulated this study. We also thank J. De Wever for improving the manuscript and two anonymous referees for very constructive comments. This work was funded by FRIA and FNRS grants. SPOT remote sensing data were provided by the European OASIS project. CNES 2001 – Spot Image distribution.

References

Adeyewa, Z. D. and Nakamura, K. 2003. Validation of TRMM radar rainfall data over major climatic regions in Africa. – J. Appl. Meteorol. 42: 331–347.

Anyamba, A. and Tucker, C. J. 2005. Analysis of Sahelian vegetation dynamics using NOAA-AVHRR NDVI data from 1981–2003. – J. Arid Environ. 63: 596–614.

Aubréville, A. 1938. La forêt coloniale: Les forêts de l'Afrique Occidentale Française. – Académie des Sciences coloniales.

Barbier, N. et al. 2006. Self-organized vegetation patterning as a fingerprint of climate and human impact on semi-arid ecosystems. – J. Ecol. 94: 537–547.

Barbier, N. et al. 2008. Spatial decoupling of facilitation and competition at the origin of gapped vegetation patterns. – Ecology 89: 1521–1531.

Barbier, N. et al. 2010. The variation of apparent crown size and canopy heterogeneity across lowland Amazonian forests. – Global Ecol. Biogeogr. 19: 72–84.

Borgogno, F. et al. 2009. Mathematical models of vegetation pattern formation in ecohydrology. – Rev. Geophys. 47: RG 1005.

Box, G. E. P. and Cox, D. R. 1964. An analysis of transformations. – J. R. Stat. Soc. Ser. B 26: 211–252.

Bryan, R. B. and Brun, S. E. 1999. Laboratory experiments on sequential scour/deposition and their application to the development of banded vegetation. – Catena 37: 147–163.

Callaway, R. M. 1995. Positive interactions among plants. – Bot. Rev. 61: 306–349.

Clos-Arceduc, M. 1956. Etude sur photographies aériennes d'une formation végétale sahélienne: la brousse tigrée. – Bull. IFAN Sér. A 7: 677–684.

Cohen, J. 1960. A coefficient of agreement for nominal scales. – Educ. Psychol. Meas. 20: 37–46.

Couteron, P. 2002. Quantifying change in patterned semi-arid vegetation by Fourier analysis of digitized aerial photographs. – Int. J. Remote Sens. 23: 3407–3425.

Couteron, P. and Lejeune, O. 2001. Periodic spotted patterns in semi-arid vegetation explained by a propagation-inhibition model. – J. Ecol. 89: 616–628.

Couteron, P. et al. 2006. Textural ordination based on Fourier spectral decomposition: a method to analyze and compare landscape patterns. – Landscape Ecol. 21: 555–567.

Deblauwe, V. 2010. Modulation des structures de végétation auto-organisées en milieu aride. – Dépt de biologie des organismes, Univ. Libre de Bruxelles.

Deblauwe, V. et al. 2008. The global biogeography of semi-arid periodic vegetation patterns. – Global Ecol. Biogeogr. 17: 715–723.

d'Herbès, J. M. et al. 1997. La brousse tigrée au Niger: synthèse des connaissances acquises. Hypothèse sur la genèse et les facteurs déterminant les différentes structures contractées. – In: d'Herbès, J. M. et al. (eds), Fonctionnement et gestion des

écosystèmes forestiers contractés sahéliens. John Libbey Eurotext, pp. 131–152.
D'Odorico, P. et al. 2006. Vegetation patterns induced by random climate fluctuations. – Geophys. Res. Lett. 33: L19404.
Eddy, J. et al. 1999. Vegetation arcs and litter dams: similarities and differences. – Catena 37: 57–73.
Elagib, N. A. 2010. Trends in intra- and inter-annual temperature variabilities across Sudan. – Ambio 39: 413–429.
Elagib, N. A. in press. Changing rainfall, seasonality and erosivity in the hyper-arid zone of Sudan. – Land Degrad. Dev.
Fisher, N. I. 1993. Statistical analysis of circular data. – Cambridge Univ. Press.
Garcia-Fayos, P. and Gasque, M. 2002. Consequences of a severe drought on spatial patterns of woody plants in a two-phase mosaic steppe of *Stipa tenacissima* L. – J. Arid Environ. 52: 199–208.
Guttal, V. and Jayaprakash, C. 2007. Self-organization and productivity in semi-arid ecosystems: implications of seasonality in rainfall. – J. Theor. Biol. 248: 490–500.
Hulme, M. 1990. The changing rainfall resources of Sudan. – Trans. Inst. Br. Geogr. 15: 21–34.
Ibrahim, F. N. 1988. Causes of the famine among the rural population of the sahelian zone of the Sudan. – GeoJournal 17: 133–141.
Kefi, S. et al. 2007a. Spatial vegetation patterns and imminent desertification in Mediterranean arid ecosystems. – Nature 449: 213–217.
Kefi, S. et al. 2007b. Local facilitation, bistability and transitions in arid ecosystems. – Theor. Popul. Biol. 71: 367–379.
Koffi, K. J. et al. 2007. Spatial pattern analysis as a focus of landscape ecology to support evaluation of human impact on landscapes and diversity. – In: Hong, S.-K. et al. (eds), Landscape ecological applications in man-influenced areas: linking man and nature systems. Springer, pp. 7–32.
Le Houérou, H. N. 1980. The rangelands of the Sahel. – J. Range Manage. 33: 41–46.
Lefever, R. and Lejeune, O. 1997. On the origin of tiger bush. – Bull. Math. Biol. 59: 263–294.
Lefever, R. et al. 2000. Generic modelling of vegetation patterns. A case study of tiger bush in sub-saharian sahel. – In: Maini, P. K. and Othmer, H. G. (eds), Mathematical models for biological pattern formation: frontiers in biological mathematics. Springer, pp. 83–112.
Lefever, R. et al. 2009. Deeply gapped vegetation patterns: on crown/root allometry, criticality and desertification. – J. Theor. Biol. 261: 194–209.
Lejeune, O. and Tlidi, M. 1999. A model for the explanation of vegetation stripes (tiger bush). – J. Veg. Sci. 10: 201–208.
Lejeune, O. et al. 1999. Short range co-operativity competing with long range inhibition explains vegetation patterns. – Acta Oecol. 20: 171–183.
Lejeune, O. et al. 2002. Localized vegetation patches: a self-organized response to resource scarcity. – Phys. Rev. E 66: 010 901R.
Lejeune, O. et al. 2004. Vegetation spots and stripes: dissipative structures in arid landscapes. – Int. J. Quantum Chem. 98: 261–271.
Ludwig, J. A. et al. 2005. Vegetation patches and runoff-erosion as interacting ecohydrological processes in semiarid landscapes. – Ecology 86: 288–297.
Mabbutt, J. A. and Fanning, P. C. 1987. Vegetation banding in arid Western Australia. – J. Arid Environ. 12: 41–59.
MacFadyen, W. A. 1950. Vegetation patterns in the semi-desert plains of British Somaliland. – Geogr. J. 116: 199–210.
Manor, A. and Shnerb, N. M. 2008. Facilitation, competition, and vegetation patchiness: from scale free distribution to patterns. – J. Theor Biol. 253: 838–842.
Meron, E. et al. 2004. Vegetation patterns along a rainfall gradient. – Chaos Solitons Fractals 19: 367–376.
Olsson, K. and Rapp, A. 1991. Dryland degradation in central Sudan and conservation for survival. – Ambio 20: 192–195.
Olsson, L. 1993. On the causes of famine drought, desertification and market failure in the Sudan. – Ambio 22: 395–403.
Olsson, L. et al. 2005. A recent greening of the Sahel – trends, patterns and potential causes. – J. Arid Environ. 63: 556–566.
Pantuliano, S. et al. 2009. Put out to pasture. War, oil and the decline of Misseriyya Humr pastoralism in Sudan. – O. D. I. Humanitarian Policy Group.
Rabus, B. et al. 2003. The shuttle radar topography mission – a new class of digital elevation models acquired by spaceborne radar. – J. Photogr. Remote Sens. 57: 241–262.
Renshaw, E. and Ford, E. D. 1984. The description of spatial pattern using two-dimensional spectral analysis. – Vegetatio 56: 75–85.
Rietkerk, M. and van de Koppel, J. 2008. Regular pattern formation in real ecosystems. – Trends Ecol. Evol. 23: 169–175.
Rietkerk, M. et al. 2002. Self-organization of vegetation in arid ecosystems. – Am. Nat. 160: 524–530.
Rietkerk, M. et al. 2004. Self-organized patchiness and catastrophic shifts in ecosystems. – Science 305: 1926–1929.
Scheffer, M. et al. 2001. Catastrophic shifts in ecosystems. – Nature 413: 591–596.
Schlesinger, W. H. et al. 1990. Biological feedbacks in global desertification. – Science 247: 1043–1048.
Serpantié, G. et al. 1992. La dynamique des états de surface d'un territoire agro-pastoral soudano-sahélien. Conséquences et propositions. – In: Le Floc'H, É. et al. (eds), L'Aridité: une contrainte au développement. Caractérisation, réponses biologiques, stratégies des sociétés. ORSTOM, pp. 419–448.
Sherratt, J. A. 2005. An analysis of vegetation stripe formation in semi-arid landscapes. – J. Math. Biol. 51: 183–197.
Sherratt, J. A. and Lord, G. J. 2007. Nonlinear dynamics and pattern bifurcations in a model for vegetation stripes in semi-arid environments. – Theor. Popul. Biol. 71: 1–11.
Sileshi, G. W. et al. 2010. Termite-induced heterogeneity in African savanna vegetation: mechanisms and patterns. – J. Veg. Sci. 21: 923–937.
Sokal, R. R. and Rohlf, F. J. 1995. Biometry: the principles and practice of statistics in biological research. – W. H. Freeman.
Thompson, S. et al. 2008. Role of biomass spread in vegetation pattern formation within arid ecosystems. – Water Resour. Res. 44: W10421.
UNEP 1992. World atlas of desertification. – Edward Arnold.
Valentin, C. and d'Herbès, J. M. 1999. Niger tiger bush as a natural water harvesting system. – Catena 37: 231–256.
Valentin, C. et al. 1999. Soil and water components of banded vegetation patterns. – Catena 37: 1–24.
von Hardenberg, J. et al. 2001. Diversity of vegetation patterns and desertification. – Phys. Rev. Lett. 87: 198101.
von Hardenberg, J. et al. 2010. Periodic versus scale-free patterns in dryland vegetation. – Proc. R. Soc. B 277: 1771–1776.
Warren, A. 1973. Some vegetation patterns in the republic of the Sudan – a discution. – Geoderma 9: 75–78.
White, L. P. 1970. Brousse Tigrée patterns in southern Niger. – J. Ecol. 58: 549–553.
Wickens, G. E. and Collier, F. W. 1971. Some vegetation patterns in the republic of the Sudan. – Geoderma 6: 43–59.
Zahran, A. M. B. 1986. Sudan rainfall variability; towards a drought assessment model. – In: Proc. Intern. Conf. on water resources needs and planning in drought prone areas, pp. 85–106.